THE JOURNAL OF COMPARATIVE NEUROLOGY 430:250–263 (2001)

Neuronal Body Size Correlates With the Number of Nucleoli and Cajal Bodies, and With the Organization of the Splicing Machinery in Rat Trigeminal Ganglion Neurons

EMMA PENA,[1] MARIA T. BERCIANO,[1] ROSARIO FERNANDEZ,[2] JOSE L. OJEDA,[1] AND MIGUEL LAFARGA[1]*

[1]Department of Anatomy and Cell Biology, Faculty of Medicine, University of Cantabria, 39011 Santander, Spain

[2]Department Physiology and Pharmacology, Faculty of Medicine, University of Cantabria, 39011 Santander, Spain

ABSTRACT

Trigeminal ganglion neurons comprise three main cell body-size types. This cell size heterogeneity provides an excellent neuronal model to study the cell size-dependent organization and dynamics of the nucleoli, Cajal (coiled) bodies (CBs), and nuclear speckles of pre-mRNA splicing factors, nuclear structures that play a key role in the normal neuronal physiology. We have analyzed the number of nucleoli and CBs and the structural and molecular organization of CBs and nuclear speckles in the three neuronal types by using immunofluorescence with antibodies that recognize nucleoli (fibrillarin), CBs (coilin), and nuclear speckles (snRNPs), confocal microscopy, and electron microscopy. Whereas the mean number of nucleoli per neuron decreases as a function of cell size, the number of CBs per cell significantly increases in large neurons in comparison with the small ones. In addition, large neurons have a higher proportion of CBs associated with the nucleolus. In all neuronal types, CBs concentrate coilin, fibrillarin, snRNPs, and the survival motor neuron protein (SMN). Immunostaining for snRNPs shows small speckle domains and extensive areas of diffuse nucleoplasmic signal in large neurons, in contrast with the large nuclear speckles found in small neurons. Furthermore, flow cytometric analysis shows that all neurons are in the range of diploid cells. These findings indicate that the fusion behavior of nucleoli, the formation of CBs and their relationships with the nucleolus, as well as the compartmentalization of the pre-mRNA splicing machinery, is related to cell body size in the trigeminal ganglion neurons. Because transcriptional activity is a basic determinant mechanism of cell size in diploid cells, we suggest that our findings reflect a distinct transcription-dependent organization of the nucleolus and splicing machinery in the three cell types of trigeminal ganglion neurons. J. Comp. Neurol. 430:250–263, 2001.

Indexing terms: survival motor neuron protein; splicing snRNPs; U2B′′; interchromatin granule clusters; nuclear speckles; DNA content

Cell sizes are intrinsically programmed and can differ greatly among cell types in metazoan organisms. Two factors, namely DNA content and transcriptional activity, are determinant mechanisms of cell size (Cavalier-Smith, 1978). In the case of vertebrate neurons, previous biochemical and flow cytometric studies support that most of the central nervous system (CNS) neurons have a constant diploid amount of nuclear DNA (Pearson et al., 1984, McIlwain, 1991; Sato et al., 1994). Consequently, differences in neuronal body size seem to be primarily determined by the transcriptional activity. Indeed, a positive correlation between cell body and total RNA synthesis has been demonstrated in frog motoneurons, indicating that large neurons need higher transcriptional activities to maintain their large size (Sato et al., 1994). The neuronal

Grant sponsor: Dirección General de Enseñanza Superior e Investigación of Spain; Grant numbers: PM96/0035, PB98-1418-C02-02; Grant sponsor: Fondo de Investigaciones Sanitarias of Spain; Grant number: FIS 00/0947; Grant sponsor: Fundacion Marqués de Valdecilla of Santander (Spain); Grant numbers: 99/3, 00/2.

*Correspondence to: Miguel Lafarga, Department of Anatomy and Cell Biology, Faculty of Medicine, University of Cantabria, Avd. Cardenal Herrera Oria s/n, 39011 Santander, Spain. E-mail: lafargam@unican.es

Received 25 May 2000; Revised 27 September 2000; Accepted 26 October 2000

transcription rate is, in turn, positively related to the magnitude of interactions between neurons and their targets, which contributes to the regulation of the soma size and metabolic activity (Goldschmidt and Steward, 1992; Magistretti, 1999). A similar relationship between transcriptional activity and cell size has been observed in nonneuronal cells. Kinetic studies of uridine incorporation rates have demonstrated that differences in cell size correspond to differences in RNA content and a tight correlation has also been shown to exist between transcription rates and RNA:DNA ratios in cells from adult rodents (Schmidt and Schibler, 1995). Moreover, the effect of transcription on cellular volume is, in turn, mediated by the accumulation of some cellular components such as ribosomes and certain proteins that have a profound influence on cell size (Macknight, 1988; Schmidt and Schibler, 1995).

Mature primary sensory ganglia neurons have been classified in three main types (A,B,C) on the basis of their size and the distribution of their organelles (Rambourg et al., 1983). Type A neurons are large neurons (40–75 μm in diameter), type B cells correspond to medium neurons (20–50 μm in diameter), whereas type C neurons are the smallest ganglion cells with a diameter of less than 20 μm (Rambourg et al., 1983). Type A and B neurons have myelinated fibers and are mainly mechanoreceptive, whereas type C give rise to largely unmyelinated fibers and are mainly nociceptive (Hunt et al., 1992; Wotherspoon and Priestley, 1999). These mature ganglion cells provide an excellent neuronal model to study the cell size-dependent organization and dynamics of three nuclear structures, i.e., nucleolus, Cajal bodies, and nuclear speckles or interchromatin granule clusters (IGCs), that play a key role in the regulation of neuronal physiology.

The nucleolus is the site of transcription of rDNA, of processing of pre-rRNA transcripts and maturation of preribosomes (for reviews, see Hadjiolov, 1985; Shaw and Jordan, 1995). It contains the ribosomal RNA (rRNA) genes, the RNA polymerase I transcription machinery and several factors involved in the processing of pre-rRNAs (for a review, see Shaw and Jordan, 1995). The coiled body was discovered by Cajal (1903) in the neuronal nucleus. It was described as a round argyrophilic "accessory body" of the nucleolus. By electron microscopy, Moneron and Bernhard (1969) rediscovered this nuclear inclusion as a tangle of coiled electron-dense threads and based on this structural configuration termed it "coiled body." Recently, coiled bodies have been renamed "Cajal bodies" in honor of the first investigator to describe them (Carvalho et al., 1999; Gall et al., 1999, Gall, 2000). The molecular analysis shows that the Cajal body (CB) is highly enriched in small nuclear and nucleolar ribonucleoproteins (snRNPs, snoRNPs) required for the maturation of both pre-mRNAs and pre-rRNAs, contains a specific marker, the p80 coilin, and shares with the nucleolus the proteins fibrillarin, Nopp 140, NAP57, and DNA topoisomerase I (for reviews, see Lamond and Carmo-Fonseca, 1993; Matera, 1999; Gall, 2000). Recently, the survival motor neurons protein (SMN) and its associated protein SIP1 (Liu and Dreyfuss, 1996; Liu et al., 1997), two factors involved in the biogenesis of spliceosomal snRNPs, have been localized in the CB (Bechade et al., 1999; Carvalho et al., 1999; Matera, 1999). The CB is interpreted as a plurifunctional organelle implicated in the biogenesis, transport, and recycling of snRNPs and snoRNPs involved in pre-mRNA splicing and pre-rRNA maturation (for a review, see Matera, 1999). The IGCs are nuclear domains devoid of DNA and composed of closely packed ribonucleoprotein particles that concentrate pre-mRNA splicing factors for their distribution to sites of active transcription (for review see Spector, 1993; Lamond and Earnshaw, 1998; Mintz et al., 1999).

In the present work, mature trigeminal ganglion neurons (TGN) were used to study whether there was any relationship between the neuronal body size and (1) the number of nucleoli, (2) the number of CBs and their relationships with the nucleolus, and (3) the structural and molecular organization of the pre-mRNA splicing machinery, particularly CBs and IGCs. Moreover, to determine whether the variation of neuronal size is related to distinct DNA content, the ploidy of neuronal types will be established by flow cytometry.

Abbreviations

CBs	Cajal (coiled) bodies
snRNPs	small nuclear ribonucleoproteins
snoRNPs	small nucleolar ribonucleoproteins
TGN	trigeminal ganglion neurons
IGCs	interchromatin granule clusters
SMN	survival motor neuron protein
SIP1	SMN-interacting protein 1
NORs	nucleolar organizer regions

MATERIALS AND METHODS

Animals

Young adult male Sprague-Dawley rats, each weighing 150–200 g, were used. The animals were anesthetized with intraperitoneal injection dose (80 mg/kg body weight) of pentobarbital. The animals were housed, supervised, and handled according to the approved national guidelines for animal care.

Transmission electron microscopy

For conventional ultrastructural examination of trigeminal ganglion neurons, the rats were perfused under deep anaesthesia with 3% glutaraldehyde in 0.1 M phosphate buffer, pH 7.4. Trigeminal ganglia were removed, rinsed in 0.1 M phosphate buffer, post-fixed in 2% osmium tetroxide, dehydrated in acetone, and embedded in araldite (Durcupan, Fluka, Buchs, Switzerland). Ultrathin sections, stained with uranyl acetate and lead citrate, were examined with a Philips EM-208 electron microscope.

Scanning electron microscopy

For scanning electron microscopy, small fragments of trigeminal ganglia fixed in 3% glutaraldehyde were squashed on a slide. The portion of the slide containing the adhered TGN was cut with a fine diamond scriber and processed for scanning electron microscopy. The samples were dehydrated in ascending grades of acetone, critical-point dried through carbon dioxide, and coated with gold/palladium in a JFC-1100 Jeol sputter coater. The samples were examined with a Philips 501 scanning electron microscope.

Light microscopy immunocytochemistry and quantification

For immunofluorescence, under deep anaesthesia the animals were perfused with 3.7% paraformaldehyde (freshly prepared from paraformaldehyde) in PBS, pH 7.4, for 15 minutes at room temperature. Trigeminal ganglia were removed, washed in PBS, and cut into small fragments. Each fragment was transferred to a drop of PBS on a siliconized slide. Then a coverslip was applied on top of the slide, and the tissue was squashed by percussion with a histologic needle to dissociate neuronal perikarya. The preparation was then frozen in dry ice, and the coverslip removed by using a razor blade. By using this procedure, most ganglion neurons remained adhered to the slide. Cell samples were processed in 96% ethanol at 4°C for 10 minutes, which increases the adhesion of cells to the slide, and rehydrated progressively in 70% ethanol and PBS. Then, the samples were sequentially treated with 0.5% Triton X-100 in PBS for 15 minutes, 0.1 M glycine in PBS containing 1% bovine serum albumin (BSA) for 30 minutes and 0.01% Tween 20 in PBS for 5 minutes. The samples were incubated for 1 hour with the primary antibody containing 1% BSA at room temperature, washed with 0.01% Tween 20 in PBS, incubated for 45 minutes in the specific secondary antibody conjugated with FITC or Texas Red (Jackson, West Grove, PA), washed in PBS, and mounted with the antifading medium Vectashield (Vector, Burlingame, CA).

The following primary antibodies were used in this study: monoclonal antibody 4G3 (Euro Diagnostica B.V., Arnhem, The Netherlands) directed against the U2B′′ snRNP (Habets et al., 1989); rabbit polyclonal serum 204.3 anticoilin (Bohmann et al., 1995); monoclonal antibody 72B9 directed against the nucleolar protein fibrillarin (Reimer et al., 1987); rabbit polyclonal serum raised against a peptide corresponding to the carboxy-terminal end of human fibrillarin (Jansen et al., 1991); human autoimmune serum D106 specific to DNA topoisomerase I (kindly provided by W. van Venrooij), and monoclonal antibodies 2B1, anti-SMN, and 2E17, anti-SIP1 (Liu and Dreyfuss, 1996; Liu et al., 1997). Samples were examined with a laser confocal microscope (BioRad MRC-1024) by using argon ion (488 nm) and HeNe (543 nm) lasers. Each channel was recorded independently and pseudocolor images were generated and superimposed. TIFF (red-green-blue) images were transferred to Adobe Photoshop for presentation. All images presented within each figure were identically adjusted for contrast, brightness, and dynamic resolution.

The quantitative analysis of the number of nucleoli and CBs, as well as that of the nuclear distribution of CBs, was performed in squash preparations, double immunolabeled with the antifibrillarin (nucleoli) and anticoilin (CBs) antibodies. Three size classes of ganglion neurons were established by using the following ranges in cell body diameter: large (larger than 40 μm), medium (20–40 μm), and small (12–20 μm). These size classes roughly corresponded to the three main types (A,B,C) of sensory ganglion neurons identified by Rambourg et al. (1983) on the basis of their size. The small cells with oval-shape nuclei (<6 μm) corresponding to glial cells were excluded from the quantitative analysis. The number of nucleoli and CBs per neuron was estimated by direct examination of the different focal planes throughout neuronal nuclei, by using a 63× oil objective and an ocular equipped with a micrometer scale. Samples of five animals were used, and at least 100 neurons for each neuronal type and animal were counted. For the quantitative analysis of the nuclear distribution of free and nucleolus-attached CBs, serial confocal sections, 0.5 μm thick, of the whole nuclei were performed in at least 100 neurons of each neuronal type. Data were analyzed by the StatView 4.5 software and by using the statistical tests ANOVA and chi square. Significance was established at $P < 0.05$.

Electron microscopy immunocytochemistry

For immunoelectron microscopy, animals were fixed with 4% paraformaldehyde in 0.12 M phosphate buffer, pH 7.4. Small segments of trigeminal ganglia were left in the same fixative for 3 hours at 4°C, dehydrated in increasing concentrations of methanol at −20°C, and embedded in Lowicryl K4M at −20°C. Ultrathin sections were sequentially incubated with 0.1 M glycine in PBS (15 minutes), normal goat serum diluted 1:100 in PBS (3 minutes), and the primary antibodies diluted in PBS containing 0.1 M glycine and 1% BSA (1 hour at room temperature). After washing, the sections were incubated with the specific secondary antibody conjugated to 10-nm or 15-nm gold particles (BioCell, Cardiff, UK) diluted 1:25 in 1% BSA in PBS (45 minutes at room temperature). After washing, the sections were stained with uranyl acetate and lead citrate. As controls, sections were treated as described but omitting the primary antibody.

Flow cytometry analysis

To analyze the intracellular DNA content, trigeminal ganglia cells were isolated by enzymatic digestion with collagenase 0.1% (Sigma, St. Louis, MO) for 30 minutes at 37°C. The cell pellets were washed twice with PBS, and the resuspended cells stained in a solution containing 100 μg/ml propidium iodide, 0.01% Triton X-100, 0.1% trisodium citrate, and 0.1 mg/ml RNAse. Samples were then washed in PBS and DNA content estimated by measuring propidium iodide fluorescence with a flow cytometer (FACS Calibur; Becton Dickinson, Franklin Lakes, NJ). Data were analyzed by using the ModFit LT software (Becton Dickinson).

RESULTS

DNA content of trigeminal ganglion neurons

Because the DNA content is one of the main determinants of cell size, first, we studied whether the variations in neuronal body size in TGN may be related to changes in DNA content. Flow cytometry analysis of propidium iodide-stained cells showed that the DNA content per cell was constant, equivalent to a diploid amount of nuclear DNA, over the range of cell body sizes studied (Fig. 1). Therefore, this DNA determination ruled out the existence of polyploidy among the population of TGN.

Squash preparations of trigeminal ganglion neurons: A reliable procedure for quantitative and cytologic studies of neuronal bodies

Squash preparations made from tissue fragments of trigeminal ganglia previously fixed in paraformaldehyde and processed as described in the Materials and Methods

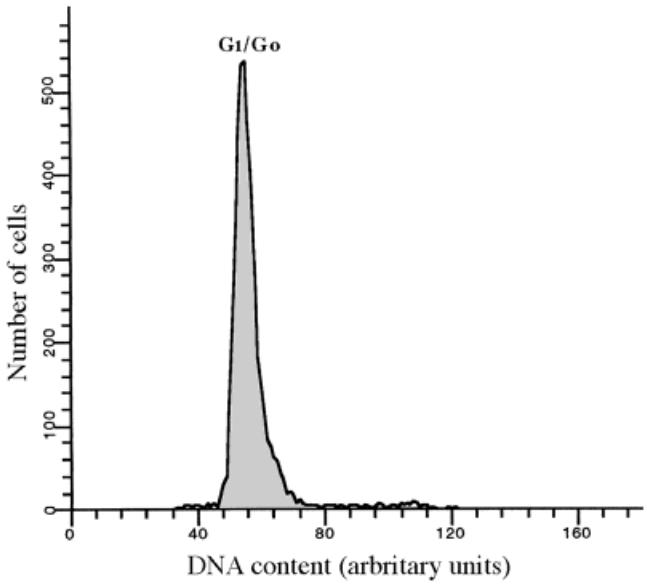

Fig. 1. DNA content distribution measured by flow cytometry in isolated trigeminal ganglion cells. The unimodal cytometric profile of sampled cells corresponds to a DNA amount in the range of diploid cells in the G1/G0 stage. The results shown are from one representative experiment of three performed with similar results.

section provided a good separation of TGN. Scanning electron microscopy examination of trigeminal ganglia samples showed typical aggregates of TGN covered by the satellite glia (Fig. 2A). When squash preparations were examined with the scanning electron microscope, isolated neuronal bodies were well-preserved and showed the heterogeneity of sizes and sometimes the emergence of a single neurite (Fig. 2B). Neuronal bodies appeared free of the glial satellite cover, and the exposed plasma membrane had false pores produced by the quick dry ice freezing of the squash preparations (Fig. 2C). It is likely that the existence of these pores of the plasma membrane facilitates the penetration of antibodies for immunofluorescence studies.

Confocal microscopy examination of squash preparations immunostained with antibodies anticoilin (Fig. 3) or antifibrillarin (Fig. 4A–C) demonstrate the excellent preservation of the morphology and organization of the CBs and nucleoli in TGN. These preparations provide a simple procedure for the quantitative analysis of the number of nucleoli and CBs in the entire nucleus by direct examination of immunofluorescence samples (Figs. 3, 4A–C). In addition, the spatial relationship between the CBs and the nucleolus can be studied by using serial confocal sections of double immunostained samples. In conclusion, the squash procedure reported here provides reliable neuronal samples on which cytologic, immunocytochemical, and quantitative analysis of neuronal bodies can be performed directly.

The number of nucleoli and CBs correlates with neuronal body size

The quantitative analysis of the mean number of nucleoli per neuron on squash preparations immunostained with the antifibrillarin antibody showed an inverse relationship between the number of nucleoli and the cell body size. Thus, as is illustrated in Table 1, the proportion of mononucleolated neurons increased from 14%, in small neurons, to 37% and 66% in medium and large neurons, respectively. Inversely, the average number of CBs per neuron, detected with the anticoilin antibody (Fig. 3), was positively related to the neuronal body size. It increased from 1.1 per nucleus, in the small neurons, to 1.8 and 2.9

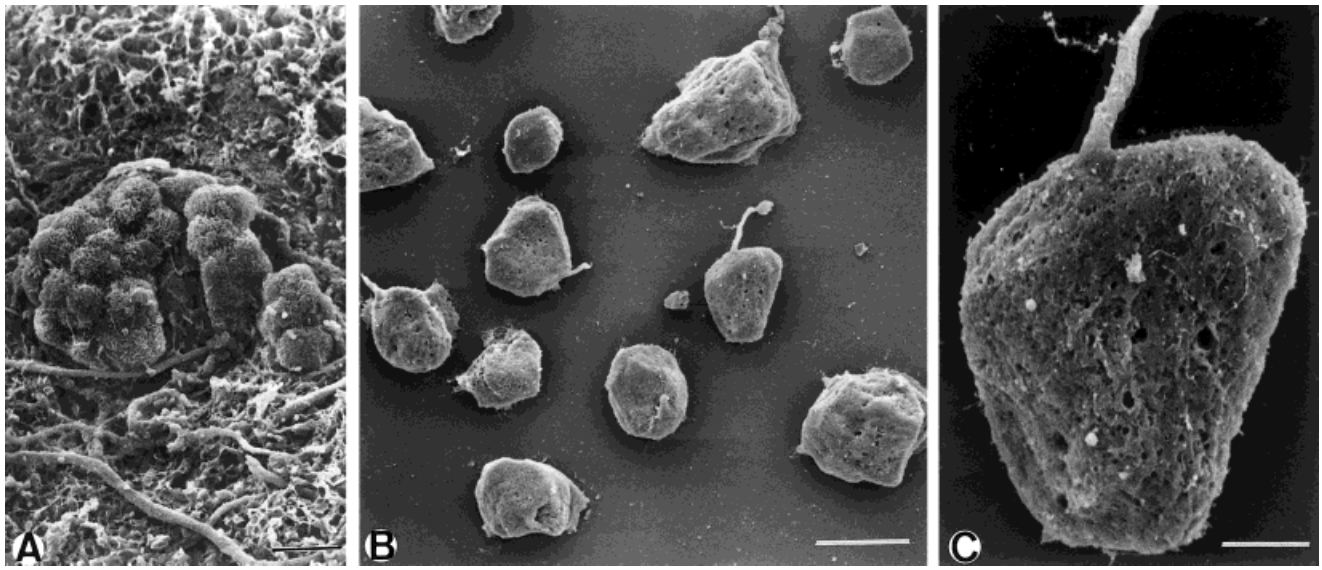

Fig. 2. Scanning electron microscopy of a squash preparation from a fragment of trigeminal ganglion. **A:** Normal cluster of nondissociated trigeminal ganglion neurons covered by the satellite glia. **B:** Dissociated neuronal bodies appear well preserved and free of their glial satellite envelope. **C:** Detail of a neuronal body with the emergence of the neurite. Note the existence of numerous false pores of the plasma membrane produced by the freezing procedure of the squash preparations. Scale bars = 25 μm in A,B; 5 μm in C.

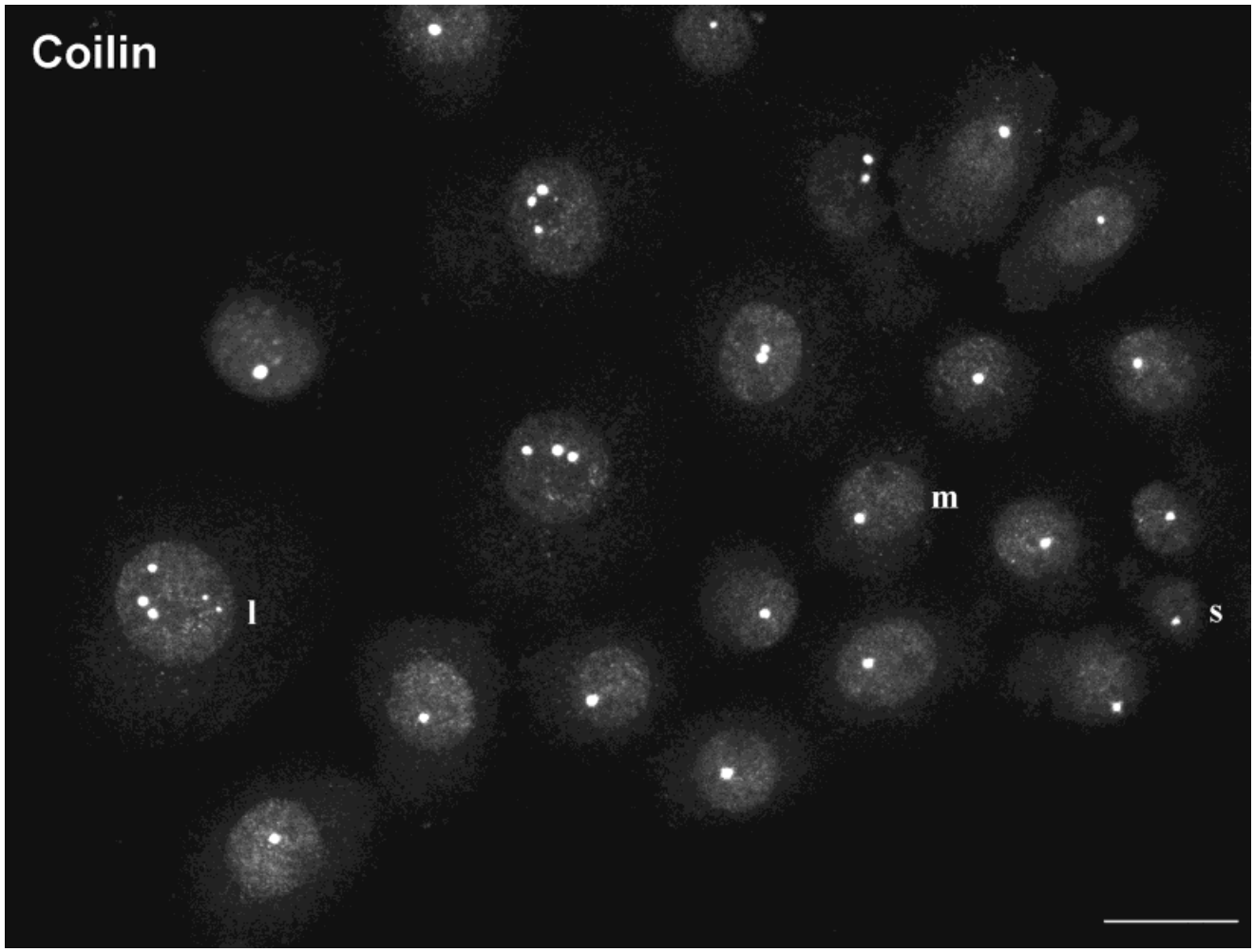

Fig. 3. Squash preparation of isolated trigeminal ganglion neurons immunostained with the anticoilin antibody. Cajal (coiled) bodies (CBs) are intensely labeled and stand out against the diffuse nucleoplasmic staining. Note a large neuron (l) with three prominent CBs and medium (m) and small (s) neurons containing a single CB. Scale bar = 20 μm.

in medium and large neurons, respectively (Fig. 4D). Differences in the pattern of spatial association of CBs with the nucleolus were found among the distinct types of TGN. Thus, the proportion of nucleolus-attached CBs was significantly higher in large neurons than in small ones (63% vs. 27%, Table 1). On the other hand, direct examination of immunostained TGN clearly showed that the nucleolar size was lower in multinucleolated than in mononucleolated neurons (Fig. 4A–C).

Neuronal CBs exhibit structural heterogeneity and different patterns of association with other nuclear organelles

The ultrastructural organization of CBs and their spatial relationships to other nuclear organelles are also issues of considerable interest. In all types of TGN, most CBs were composed of both granules and dense coiled threads and an intervening lower density matrix (Fig. 5A–E), as previously reported in other neuronal types (Kinderman and LaVelle, 1976; Hervas et al., 1980; Lafarga et al., 1983). An important structural variation was the occurrence in a few neurons of a segregated CB with a separated mass of dense fibrillar material. This type of CB variant was sometimes in close proximity to the nucleolar surface, and the segregated mass seemed to be a portion of the dense fibrillar component of the nucleolus extruded from the nucleolar surface and incorporated into the CB (Fig. 5B). A second variant was a bipartite CB that consisted of a typical CB accompanied by a juxtaposed mass of homogeneous texture and lower electron density (Fig. 5E).

Regarding the spatial relationships of CBs with other nuclear organelles in TGN, the ultrastructural analysis confirmed the frequent occurrence of CBs attached to the nucleolar surface, particularly in the large neurons. The dense coiled threads of these CBs were in direct continuity with portions of the dense fibrillar component of the nucleolus at the nuclear periphery (Fig. 5A,B). Apart from the nucleolus, CBs were frequently observed in close proximity to IGCs or even partially surrounded by them (Fig.

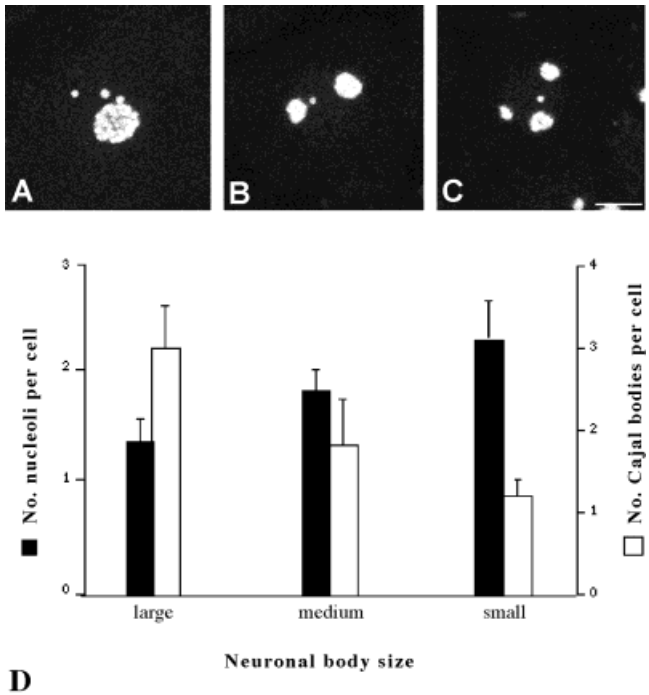

Fig. 4. Distribution of nucleoli and Cajal bodies (CBs) in the three cell-size types of trigeminal ganglion neurons (TGN). A–C: Representative examples of large (**A**), medium (**B**), and small (**C**) neurons immunostained with the antifibrillarin antibody. Both nucleoli and CBs appear specifically labeled. Note the presence of a single, large nucleolus and three CBs in the large neuron (A), two nucleoli and a CB in the medium neuron (B), and three nucleoli and a CB in the small neurons (C). **D:** Distribution of nucleoli and CBs in the three types of TGN. Bars represent means ± standard deviation of the mean. Significant differences were detected when the number of nucleoli or CBs per cell was compared among the three types of TGN (large vs. small neurons, $P < 0.001$; large vs. medium neurons and medium vs. small neurons, $P < 0.05$). Scale bar = 5 μm for A–C.

5C). Associations of CBs with nuclear rods formed by densely packed microfilaments were also observed (Fig. 5D). Another association of the CBs was with a distinct nuclear body composed of an aggregate of fine coiled fibrils, approximately 20 nm in diameter. This nuclear body, of smaller size and lower electron density than the CB, was sometimes found near the CB but never in direct continuity with it (Fig. 5D).

Molecular characterization of CBs in trigeminal ganglion neurons

Next, we examined by immunofluorescence and confocal laser microscopy the distribution of molecular constituents of CBs in the different types of TGN. Our results indicated that CBs concentrated components characteristic of mature CBs in the three types of neurons. Thus, double-labeling experiments showed a strong colocalization of coilin with fibrillarin, DNA topoisomerase I, SMN and its associated protein SIP 1, and snRNPs in all CBs analyzed (Fig. 6A–O). Gemini of CBs or gems independent of CBs (Liu and Dreyfuss, 1996) were not detected with the anti-SMN or anti-SIP1 antibodies. To investigate the ultrastructural localization of CB components, immunoelectron microscopy was performed by using antibodies

TABLE 1. Percentage of Neurons With Single or Multiple Nucleoli (No) and With Free or Nucleolus-Attached CBs in the Different Types of TGN[1]

	Number of nucleoli (No)				Cajal bodies (CBs)	
Neuron size	% 1 No	% 2 No	% 3 No	% 4–6 No	% Free CBs	% No-attached CBs
Small	14	41	32	13	73	27
Medium	37	43	16	4	47	53
Large	66	29	5	—	37	63

[1]$P < 0.001$. Both the number of nucleoli and the spatial distribution of CBs are dependent on neuronal body size.

directed against coilin, U2B″, a splicing snRNP protein that is known to be highly concentrated in CBs (Carmo-Fonseca et al., 1992), and fibrillarin. With the anticoilin antibody, the results showed that both nucleolus-attached and free CBs were strongly decorated with gold particles, particularly on the dense coiled threads (Fig. 7A–C). In the segregated form of CBs, gold particles decorated the coiled threads and the border of the dense fibrillar masses but not their insides (Fig. 7D). Similarly, the U2B″ antibody immunostained CBs, excluding the segregated portion of dense fibrillar material (Fig. 7E,F). Immuno-gold detection of fibrillarin revealed the typical pattern of distribution on the dense fibrillar component of the nucleolus and coiled threads of normal CBs (Fig. 7G). Interestingly, fibrillarin was highly concentrated on the dense fibrillar masses of segregated CBs (Fig. 7I), supporting the view that these masses are portions of the dense fibrillar component of the nucleolus extruded from the nucleolar surface. However, fibrillarin was conspicuously absent on the juxtaposed part of homogeneous texture and lower electron density of bipartite CBs (Fig. 7H).

The organization of nuclear speckles containing snRNP splicing factors is related to neuronal body size

Having established that the number of CBs per neuron increases as a function of neuronal body size, we next examined the organization of the IGCs in the different types of TGN by electron microscopy (Fig. 8). The IGCs appeared composed of closely packed interchromatin granules, 20–25 nm in diameter (Fig. 9A). Within a given IGC, the distribution of the interchromatin granules was not homogeneous and areas with different degrees of aggregation were seen. In addition, some IGCs exhibited small aggregates of dense fibrogranular material, ranging in size from 85 to 150 nm, which were intermingled with the interchromatin granules (Fig. 9B).

By direct examination of ultrathin sections, different patterns of organization of IGCs were seen in the three types of TGN. Thus, cell nuclei of large neurons, characterized by their prominent nucleoli and a dispersed chromatin configuration, showed several very small IGCs in ultrathin sections (Fig. 8A). In medium neurons, a few well-defined IGCs of larger size were clearly distinguishable from the nucleoplasm (Fig. 8B), whereas the largest IGCs were frequently observed in small neurons (Fig. 8C). Because IGCs are the ultrastructural counterpart of the nuclear speckles enriched in pre-mRNA splicing factors (for review see Spector, 1993; Lamond and Earnshaw, 1998), we next investigated whether the different organization of IGCs in the three neuronal types correlates with the distribution of the snRNPs splicing factors immuno-

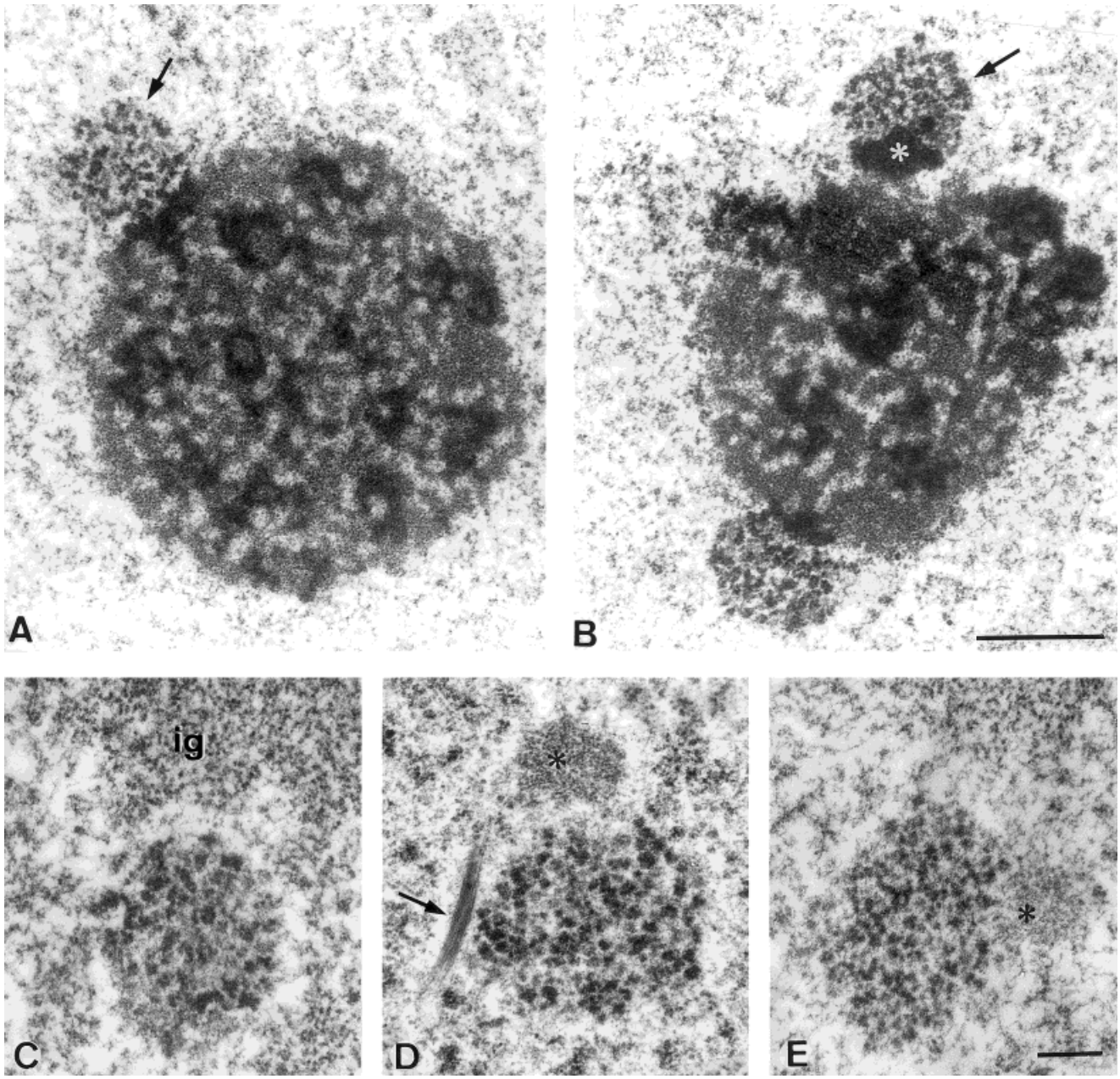

Fig. 5. Electron photomicrographs of Cajal bodies (CBs) attached to the nucleolus (A,B) and spatially related to other nuclear structures (C–E). **A:** The dense coiled threads of this CB (arrow) are in direct continuity with the dense fibrillar component at the nucleolar surface. Note the typical reticulated configuration of the nucleolus with its granular and dense fibrillar components. **B:** A CB (arrow) appears with a segregated mass of dense material (asterisk) in close proximity to the nucleolar surface. **C:** This CB is partially surrounded by a cluster of interchromatin granules (ig). **D:** Associations of a nuclear rod (arrow) and a smaller nuclear body (asterisk) with a typical CB. **E:** Bipartite CB composed of a larger portion of both granules and coiled threads and a juxtaposed part of amorphous lower density material (asterisk). Scale bar = 1 μm for A,B; 3 μm for C–E.

stained with the anti-U2B″ antibody. In large neurons, snRNPs were diffusely distributed in extensive nucleoplasmic areas, in addition to being localized in small irregular speckles and CBs (Fig. 10A). By contrast, a few larger nuclear speckles appeared intensely immunostained with the anti-snRNPs antibody in medium and small neurons (Fig. 10B,C).

DISCUSSION

We have taken advantage of the cell size heterogeneity of TGN to address the question of a possible relationship between neuronal body size and organization of both nucleoli and pre-mRNA splicing machinery in these cells. In summary, our results indicate that neuronal body size

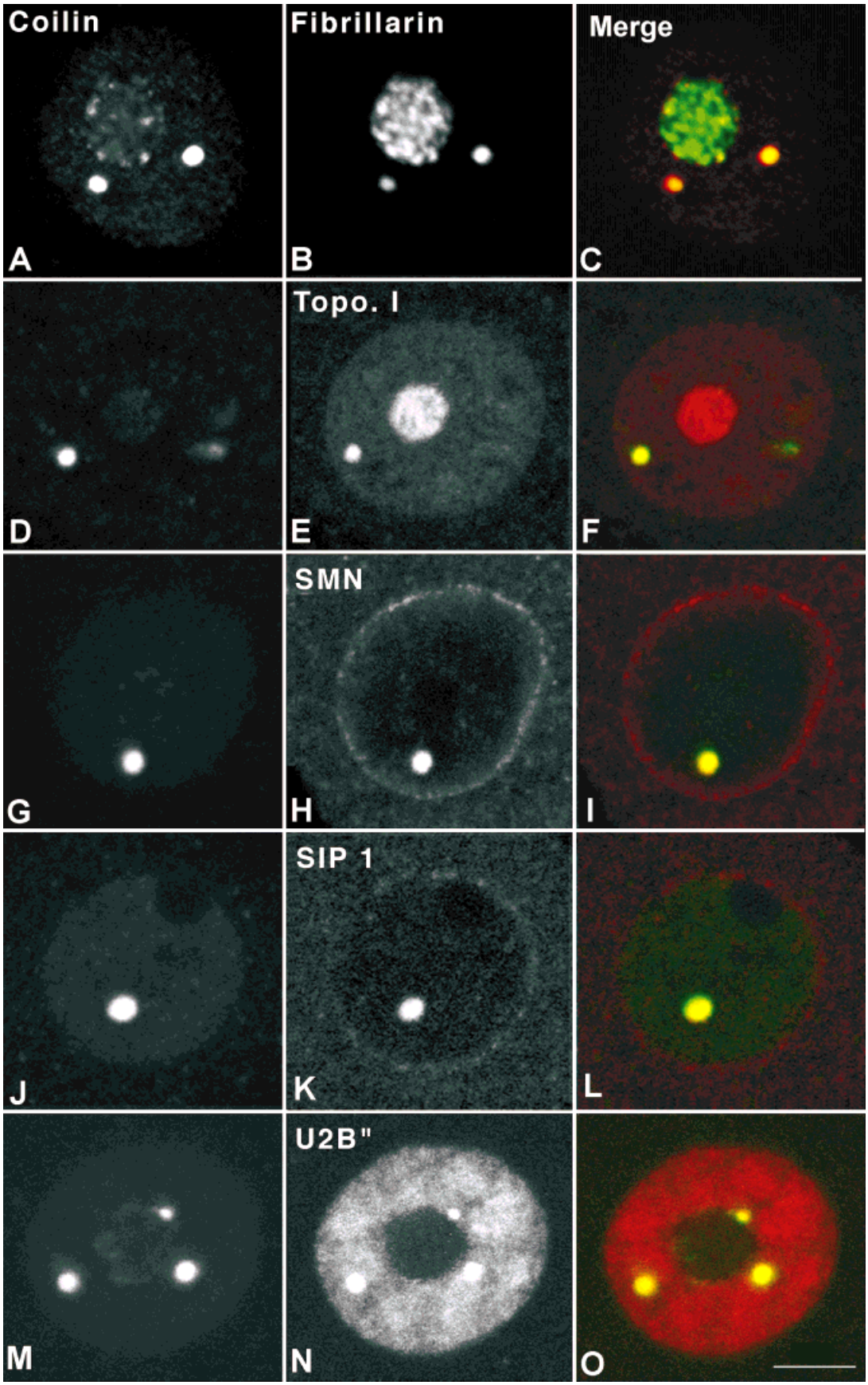

Figure 6 (Overleaf)

correlates with the number of nucleoli and CBs per neuron, with the pattern of association between these two nuclear organelles, and with the compartmentalization of splicing snRNPs within the cell nucleus. Moreover, our flow cytometric analysis indicates that TGN are diploid cells, ruling out the variations in the DNA content as a determinant mechanism of different neuronal body sizes. Because cell size is positively related to transcriptional activity in CNS neurons and in other diploid cell types (McIlwain, 1991; Sato et al., 1994; Schmidt and Schibler, 1995), we suggest that the level of transcriptional activity plays a key role in the organization pattern of nucleoli, CBs, and pre-mRNA splicing machinery in the different types of TGN.

The number of nucleoli is inversely related to the neuronal body size

Squash preparations of TGN immunostained with the antifibrillarin antibody provide a simple reliable method of counting the exact number of nucleoli per cell in the entire neuronal nucleus. Our results show that neuronal body size is related to the mean number of nucleoli per cell, resulting in a significant increase in the frequency of mononucleolated cells in large neurons compared with medium and small neurons.

It is well known that the maximum number of nucleoli per cell is determined by the number of chromosomes carrying ribosomal RNA genes (McClintock, 1934). These genes are arranged in tandem repetitions at the chromosomal nucleolar organizer regions (NORs), each of which may direct the formation of a nucleolus (for a review, see Schwarzacher and Wachtler, 1993). Previous genetic studies have demonstrated that diploid cells of the rat have six NORs (Kano et al., 1976) and our flow cytometric analysis of DNA content indicates that TGN are diploid cells, resulting in a theoretical maximum number of six nucleoli per neurons. The lower number of nucleoli found in TGN may be explained by the fusion of NORs and nucleoli during neuronal differentiation, giving rise to nucleolus carrying more than one NOR. Thus, a progressive decrease in the number of nucleoli has previously been demonstrated during differentiation of several neuronal types (Buschmann and LaVelle, 1981; Crespo et al., 1988; Lafarga et al., 1995; Hatton and von Bartheld, 1999) and nonneuronal cells (Schwarzacher and Wachtler, 1993). The degree of NOR association is also dependent on the duration of cell cycle, and nondividing cells such as mammalian neurons display only one or a few nucleoli (Schwarzacher and Wachtler, 1993). Importantly, the present results in TGN indicate that the fusion pattern of NORs in a single or multiple nucleoli is also related to neuronal size, with the highest tendency of NORs to fuse being in large neurons. This fact raises the possibility that the fusion behavior of NORs might be regulated by the transcriptional activity of maturing neurons. This would result in the predominance of a single nucleolus in large neurons (higher transcriptional activity) and of multiple nucleoli in small neurons (lower transcriptional activity). Several lines of investigation indicate that cellular size is positively related to transcriptional activity and large cells accumulate more RNA per unit of DNA than smaller cells to support their greater size and cellular activity (McIlwain, 1991; Sato et al., 1994; Schmidt and Schibler, 1995). In particular, the accumulation of ribosomes produced by nucleolar transcription (Hadjiolov, 1985), together with protein concentration, are thought to be the main determinants of cell volume (Macknight, 1988; Schmidt and Schibler, 1995). In this context, the formation of only one nucleolus in the majority of large TGN may be an adaptive cellular mechanism to facilitate the recruitment of active ribosomal genes and the molecular machinery for rRNA transcription and processing in a unique nuclear domain. This process might increase the efficiency of the ribosome biogenesis.

The number of CBs and their relationships with the nucleolus correlate with neuronal body size

Our quantitative analysis of the number of CBs in TGN shows that the number of CBs significantly increases from small to large neurons. This finding indicates that the formation of CBs is directly related to the neuronal body size and also supports that CBs are transcription-dependent nuclear organelles. This interpretation is consistent with the observation that CBs are more abundant in rapidly growing and stimulated cells in cultures (for reviews, see Lamond and Carmo-Fonseca, 1993; Spector, 1993). Similarly, in supraoptic nucleus neurons in vivo, the neuronal body size and the number of CBs increase after a sustained up-regulation of transcription induced by chronic osmotic stimulation (Modney and Hatton, 1989; Lafarga et al., 1991). On the contrary, the number of CBs decreases in supraoptic neurons when transcriptional activity is dramatically inhibited during the early neuronal response to osmotic stress (Lafarga et al., 1998). Additional data supporting the dynamic nature of CBs come from the observation that the disruption of transcription and rRNA processing induced by axotomy is associated with a substantial reduction in the number of CBs (Haggar, 1957; Clark et al., 1991). This reduced incidence of CBs after axotomy is accompanied by nucleolar changes that are similar to those observed during experimental rRNA down-regulation in other cell types (Clark et al., 1991). Although the functions of CBs are not completely understood, the high concentration of splicing snRNPs and some nucleolar proteins in CBs has led to the suggestion that they play a main role in the biogenesis, transport, or recycling of splicing factors and some nucleolar constituents (for reviews, see Carvalho et al., 1999; Matera, 1999; Sleeman and Lamond, 1999). In this context, the variations in the number of CBs observed in TGN may possibly be related to distinct requirements of pre-mRNA splicing factors and ribosome biogenesis in these neurons, depending on cell size and metabolic activity.

The present study shows differences not only in the number of CBs but also in their frequency of association with the nucleoli in the three cell types of TGN, with the

Fig. 6 (Overleaf). Confocal microscopy images representative of trigeminal ganglion neurons (TGN) double stained with coilin and fibrillarin (**A–C**), coilin and DNA topoisomerase I (**D–F**), coilin and survival motor neuron protein (SMN) (**G–I**), coilin and SMN-interacting protein 1 (SIP1) (**J–L**), and coilin and U2B′′ (**M–O**). Coilin colocalizes with the other studied components in all Cajal bodies. Note the staining of the nucleolus with the antifibrillarin (B) and anti-DNA topoisomerase I antibodies (E) and the staining of the nuclear envelope with the anti-SMN antibody (H). Scale bar = 5 μm for A–O.

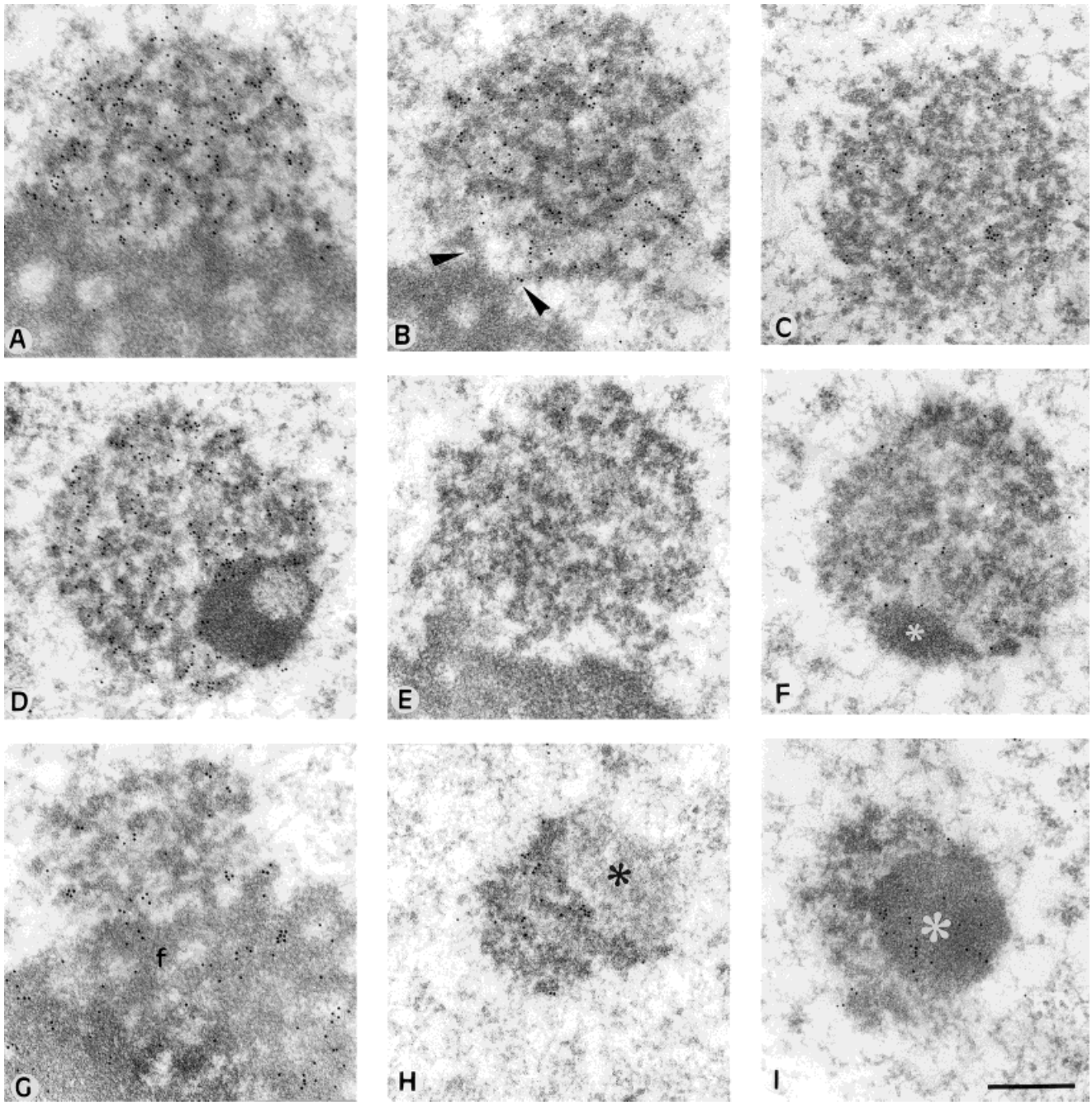

Fig. 7. Immunoelectron localization of coilin (A–D), small nuclear ribonucleoproteins (snRNPs) (E,F) and fibrillarin (G–I) in Cajal bodies (CBs) of trigeminal ganglion neurons. **A–D:** With the anticoilin antibody a high density of immuno-gold particles specifically decorated the dense coiled threads of CBs. In A, an extensive portion of the CB is directly apposed on the dense fibrillar component of the nucleolus, whereas the CB of B maintains a minimal connection with this nucleolar component (arrowheads), and the CB of C appears free into the nucleoplasm. D illustrates a segregated CB with a dense fibrillar mass containing a small pale area. The inside of this mass is devoid of coilin immunolabeling. **E,F:** Coiled threads of CBs immuno-gold labeled with the anti-U2B′′ antibody. In F, the segregated dense mass (asterisk) is devoid of immunolabeling. **G–I:** Nucleolar and CB distribution of fibrillarin. In G, the dense fibrillar component of the nucleolus (f) and the coiled threads of the nucleolus-attached CB appear stained with the antifibrillarin antibody. The image in H shows a bipartite CB with gold-labeled coiled threads and unlabeled amorphous mass (asterisk). In I, the prominent dense mass (asterisk) of a segregated CB is decorated with gold particles of fibrillarin immunolabeling. Scale bar = 0.3 μm for A–I.

large type exhibiting the highest proportion of nucleolus-attached CBs. This association has been reported in many neuronal types at light and electron microscopy levels (Hardin et al., 1969; Kinderman and LaVelle, 1976; Lafarga et al., 1983; Raska et al., 1990; Peters et al., 1991; Janevski et al., 1997) and is mediated by direct continuity

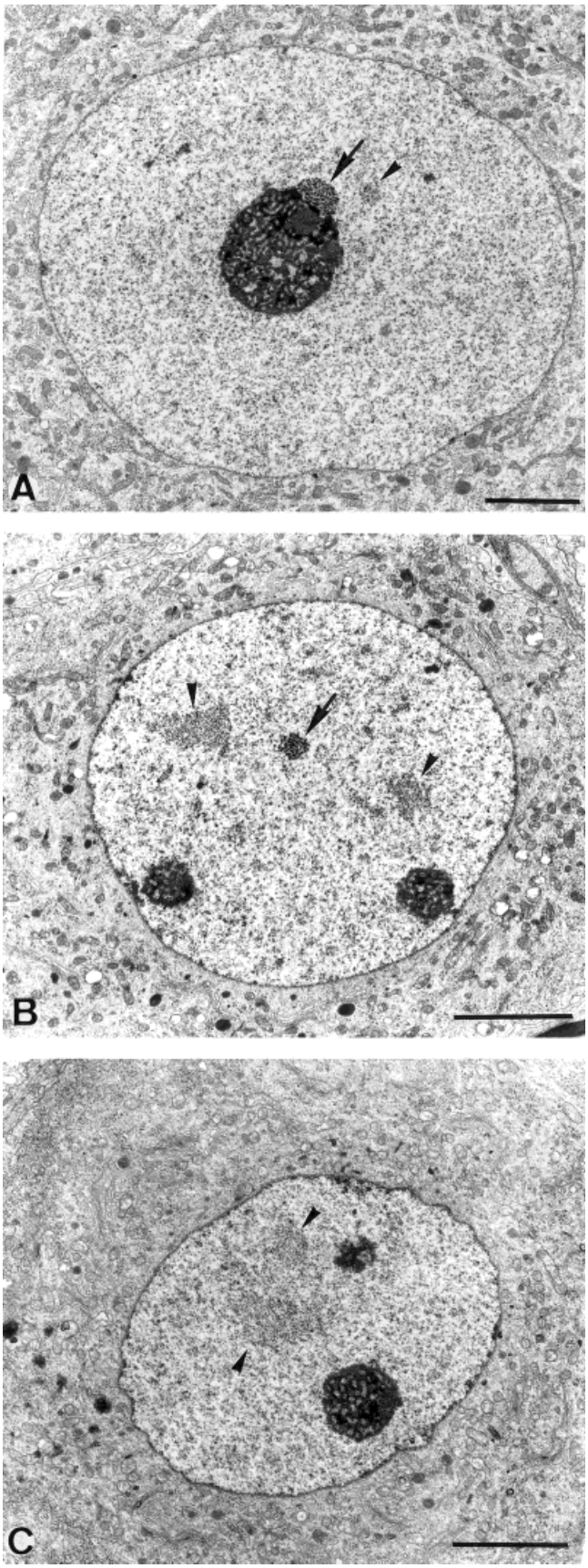

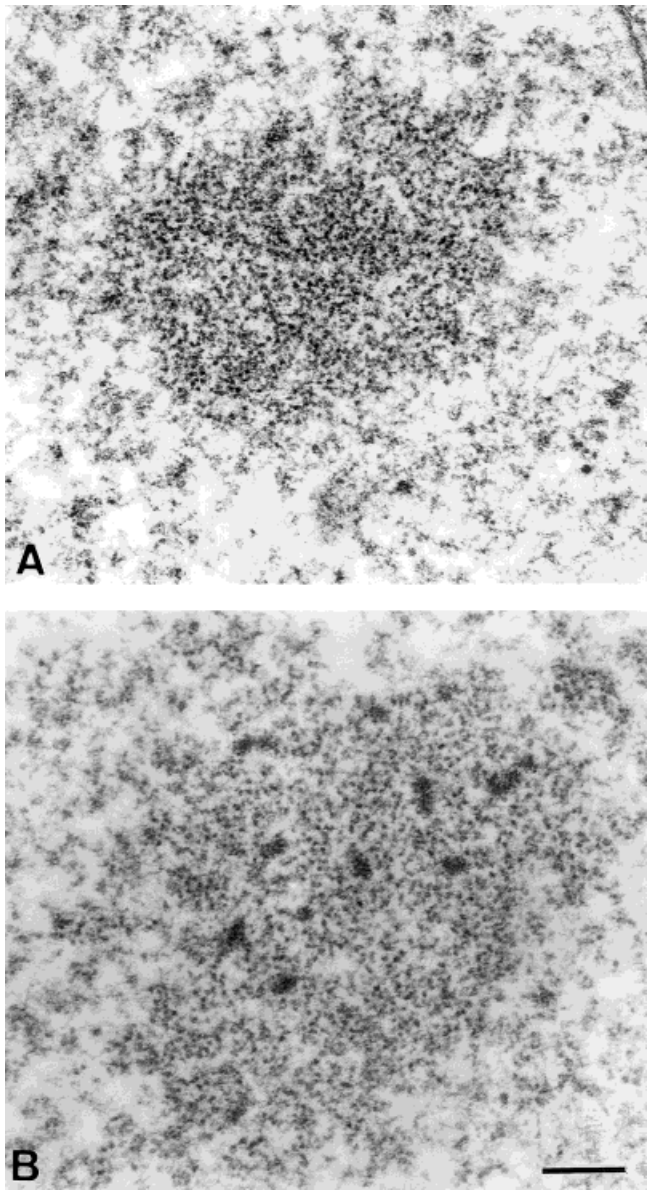

Fig. 9. Detail of interchromatin granule clusters (IGCs) from medium trigeminal ganglion neurons. **A:** An IGC uniquely composed of closely packed interchromatin granules. **B:** This IGC contains several small dense aggregates that appear intermingled with the granules. Scale bar = 0.3 μm for A,B.

between the dense coiled threads of CBs and the dense fibrillar component of the nucleolar periphery. The structural link between CBs and nucleoli, as well as our previ-

Fig. 8. Electron photomicrograph of the cell nucleus from a large (**A**), medium (**B**), and small (**C**) trigeminal ganglion neurons. The nucleus of A shows a prominent nucleolus with an associated Cajal body (CB) (arrow), extensive areas of dispersed chromatin, and small interchromatin granule clusters (IGCs) (arrowhead). In B, the smaller nucleus displays two nucleoli, a free CB (arrow), and two large IGCs (arrowheads). The image in C illustrates the nucleus of a small neuron with two nucleoli and prominent IGCs (arrowheads). Scale bar = 3 μm for A–C.

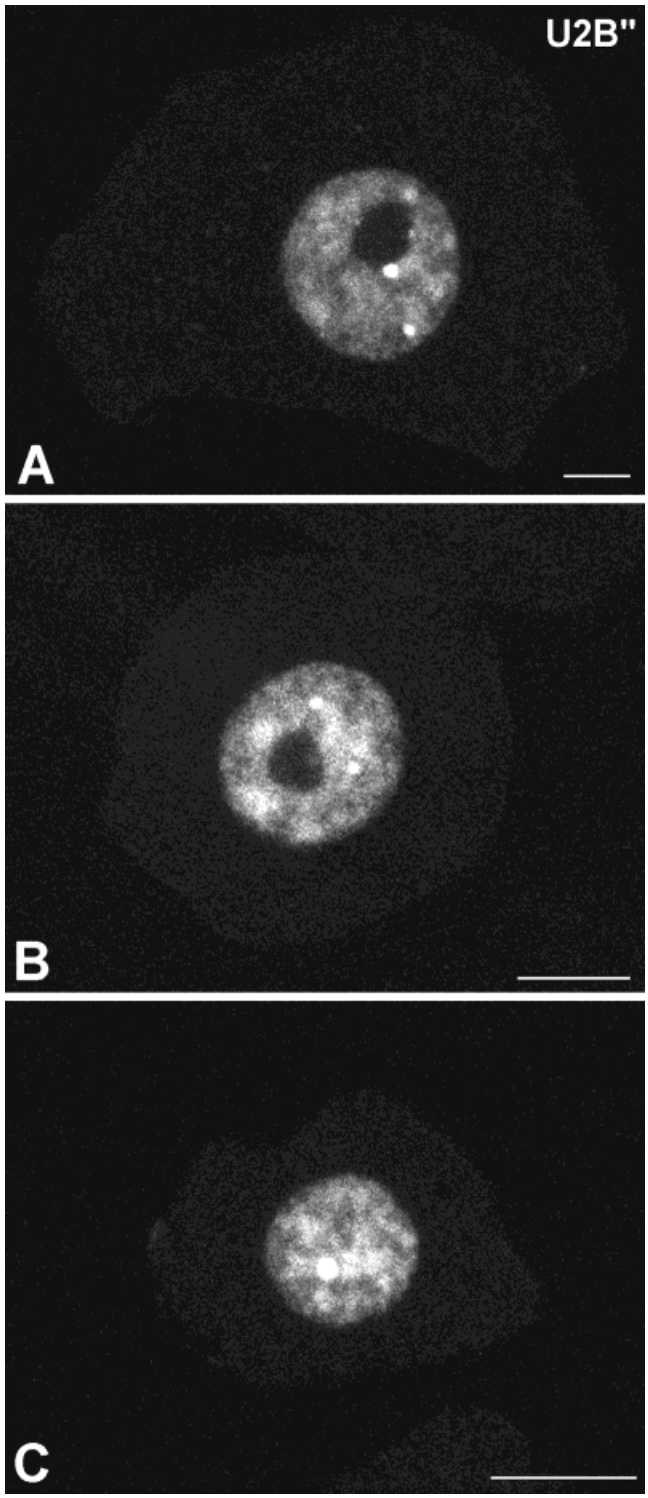

Fig. 10. Confocal microscopy images of representative large (**A**), medium (**B**), and small (**C**) trigeminal ganglion neurons immunostained with the anti-U2B′′ antibody for the demonstration of small nuclear ribonucleoproteins. The cell nucleus of the large neuron (A) shows two intensely labeled Cajal bodies (CBs) and a diffuse nucleoplasmic labeling. In the medium neuron (B), prominent nuclear speckles with two associated CBs appear intensely labeled around the unstained nucleolus. The image in C illustrates a small neuron with a large CB and prominent irregular speckle domains intensely immunostained. Scale bars = 10 μm for A–C.

ous observation of a perinucleolar accumulation of CB precursors after inhibition of transcription (Lafarga et al., 1998), supports the view that CBs can be assembled at the nucleolar surface in a transcription-dependent manner. That the association of CBs with the nucleolus may reflect dynamic interactions between both organelles is also suggested by the accumulation in CBs of typical nucleolar constituents, such as the proteins fibrillarin (Raska et al., 1990; present results), Nopp 140 and NAP57 (Meir and Blobel, 1994), and the U3 and U8 snoRNPs, all of them involved in pre-rRNA processing (for a review, see Gall, 2000). In this scenario, the higher number of CBs and their frequent associations with the nucleolus observed in large TGN could certainly facilitate the targeting to the nucleolus of basic constituents of the pre-rRNA processing machinery in neurons with high cytoplasmic requirements for ribosome biogenesis.

Structural and molecular organization of CBs

The present immunocytochemical results indicate that CBs have similar composition and contain basic constituents of mature CBs in all types of TGN. Such components include the CB marker coilin, the nucleolar proteins fibrillarin and DNA topoisomerase I, and snRNPs involved in the splicing of pre-mRNAs. Furthermore, the SMN protein and its associated factor SIP1 always colocalize with coilin in all CBs examined. The SMN is encoded by the survival motor neuron gene, which is mutated in approximately 98% of the patients with spinal muscular atrophy (Lefebvre et al., 1998). Recent experimental evidences indicate that the SMN protein is involved in the cytoplasmic assembly of snRNPs (Fisher et al., 1997) and might also participate in nuclear snRNP function (for a review, see Matera, 1999). Originally, the SMN protein was localized in distinct nuclear bodies called Gemini of CBs or gems due to their close association with CBs (Liu and Dreyfuss, 1996). However, there has been some controversy over whether gems and CBs colocalize or exist as independent nuclear bodies (for a review, see Young et al., 2000). In the present study, SMN and SIP1 are always localized in CBs of TGN, as occurs in other cell types (Bechade et al., 1999; Carvalho et al., 1999; Matera, 1999; Young et al., 2000). This colocalization is consistent with our previous results (Carvalho et al., 1999) indicating that in the biogenesis pathway of splicing snRNPs there is a nuclear flux of snRNPs, accompanied by the SMN protein, through the CBs.

Regarding the ultrastructural organization of CBs, the majority of CBs in trigeminal ganglion neurons present the typical morphology of dense coiled threads (Kinderman and LaVelle, 1976; Hervas et al., 1980; Lafarga et al., 1983; Clark et al., 1990), in which coilin, fibrillarin, and snRNPs appear concentrated by immunoelectron microscopy (Raska et al., 1990; Lafarga et al., 1998; present results). However, the molecular composition of the second structural component of the CB, the intervening lower density matrix, remains to be clarified.

Independently of the neuronal type, we have found two structural CB variants in a few CBs: segregated and bipartite CBs. Concerning the segregated CB, the present study indicates that its dense segregated mass has a fine structure and composition very similar to that of the dense fibrillar component of the nucleolus, as indicated by the high concentration of fibrillarin in both structures. Re-

cently, there is some controversy over whether CBs can emerge from the nucleolus or fuse to it (for reviews, see Matera, 1999; Sleeman and Lamond, 1999). However, in the case of segregated CBs, the structural and molecular similarities between the dense segregated mass of the CB and the fibrillar component of the nucleolus, along with our observation of these CBs attached to the nucleolus, support the view that some CBs can bud off the nucleolar surface and move into the nucleoplasm. The second variant of CBs is a bipartite CB that in addition to the coiled threads has an associated mass of low density amorphous material, which lacks basic constituents of the coiled threads such as coilin, fibrillarin, and snRNPs. We have reported this type of CB in supraoptic neurons (Lafarga et al., 1998), and the molecular characterization of the juxtaposed mass of amorphous material remains to be established.

The organization of the splicing machinery is related to neuronal body size

Our immunocytochemical study of the localization of snRNPs with the anti-U2B″ antibody shows small speckle domains and a more diffuse nucleoplasmic distribution of splicing snRNPs in large neurons, in comparison with small and medium neurons, in which a few larger nuclear speckles appear. The distinct localization patterns of snRNPs observed in the different types of TGN are in total agreement with the cell-size variations in the distribution of IGCs detected by electron microscopy analysis. In addition, we have identified structural subdomains formed by small aggregates of dense fibrogranular material in some IGCs. Similar aggregates have been reported during maturation of facial neurons (Jones and LaVelle, 1986). Although we have not investigated the molecular constituents of these subdomains, they are likely related to the subspeckles enriched in certain splicing factors recently reported in culture cells by immunofluorescence (Mintz and Spector, 2000).

Several lines of investigation indicate that IGCs represent the ultrastructural counterpart of the nuclear speckles enriched in components of the pre-mRNA splicing machinery (for reviews, see Spector, 1993; Lamond and Earnshaw, 1998; Mintz et al., 1999). IGCs contain little to no DNA, and they are not nuclear domains of active transcription (for a review, see Spector, 1993). By visualizing the nuclear dynamic of the splicing factor ASF fused to GFP in living cells, Misteli et al. (1997) have demonstrated that nuclear speckles are dynamic depots implicated in the supply of splicing factors to active sites of transcription. The close relationship between the organization of nuclear speckles and the transcriptional activity is also supported by experimental studies indicating that, in actively transcribing cells, splicing factors are predominantly dispersed throughout the nucleoplasm; and these factors relocate in a few large speckle domains in poorly transcribing cells or after inhibition of either transcription or splicing (for reviews, see Spector, 1993; Zeng et al., 1997: Berciano et al., 1999). In this scenario, the predominantly diffuse distribution of snRNPs in large TGN may reflect that in neurons with high transcriptional activity a great proportion of splicing snRNPs are recruited at active transcription sites throughout the dispersed euchromatin domains. By contrast, in small and medium TGN, with lower transcriptional activity, a considerable amount of snRNPs remain stored in nuclear speckle domains or IGCs. In fact, we have recently demonstrated that the transcription factor c-Jun localizes in euchromatin domains of TGN but is conspicuously absent in nuclear speckles (Pena et al., 2000). We conclude that the nuclear compartmentalization of splicing snRNPs and the organization of IGCs in TGN is cell size-dependent and is related to the transcriptional activity of these cells.

ACKNOWLEDGMENTS

We thank Mrs. Raquel Garcia Ceballos for technical support. We also thank Prof. G. Dreyfuss (University of Pennsylvania, Philadelphia, PA) for generously providing 2B1 (anti-SMN) and 2E17 (anti-SIP1) antibodies; Angus I. Lamond (University of Dundee, Dundee, UK) for anticoilin rabbit serum 204.3 and antifibrillarin 72B9 monoclonal antibody; Prof. Maria Carmo-Fonseca (University of Lisbon, Lisbon, Portugal) for antifibrillarin rabbit serum; and Prof. W. van Venrooij (University of Nijmengen, Nijmengen, The Netherlands) for the anti-DNA topoisomerase I human autoimmune serum D106.

LITERATURE CITED

Bechade C, Rostaing P, Cisterni C, Kalisch R, La Bella V, Pettmann B, Triller A. 1999. Subcellular distribution of survival motor neuron (SMN) protein: possible involvement in nucleocytoplasmic and dendritic transport. Eur J Neurosci 11:293–304.

Berciano MT, Fernandez R, Pena E, Calle E, Villagra NT, Lafarga M. 1999. Necrosis of Schwann cells during tellurium-induced primary demyelination: DNA fragmentation, reorganization of splicing machinery, and formation of intranuclear rods of actin. J Neuropathol Exp Neurol 58:1234–1243.

Bohmann K, Ferreira J, Lamond AI. 1995. Mutational analysis of p80 coilin indicates a functional interaction between coiled bodies and the nucleolus. J Cell Biol 131:817–831.

Buschmann MB, LaVelle A. 1981. Morphological changes of the pyramidal cell nucleolus and nucleus during development and aging. Mech Ageing Dev 15:385–397.

Cajal SR. 1903. Un sencillo método de coloración selectiva del retículo protoplasmático y sus efectos en los diversos órganos nerviosos de vertebrados e invertebrados. Trab Lab Invest Biol 2:129–221.

Carmo-Fonseca M, Pepperkock R, Carvalho MT, Lamond AI. 1992. Transcription-dependent colocalization of the U1, U2, U4/U6 and U5 snRNPs in coiled bodies. J Cell Biol 117:1–14.

Clark P, Jones KJ, LaVelle A. 1990. Ultrastructural and morphometric analysis of nucleolar and nuclear changes during the early growth period in hamster facial neurons. J Comp Neurol 302:749–760.

Clark P, Jones KJ, LaVelle A. 1991. Ultrastructural changes in the nucleolus of facial motor neurons following axotomy during an early critical period in development. J Comp Neurol 312:132–144.

Carvalho T, Almeida F, Calapez A, Lafarga M, Berciano MT, Carmo-Fonseca M. 1999. The spinal muscular atrophy disease gene product, SMN: a link between snRNP biogenesis and the Cajal (coiled) body. J Cell Biol 147:715–727.

Cavalier-Smith T. 1978. Nuclear volume control by nucleoskeletal DNA, selection for cell volume and cell growth rate, and the solution of the DNA c-value paradox. J Cell Sci 34:247–278.

Crespo D, Viadero CF, Villegas J, Lafarga M. 1988. Nucleoli numbers and neuronal growth in supraoptic nucleus neurons during postnatal development in the rat. Brain Res Dev Brain Res 44:151–155.

Fisher U, Liu Q, Dreyfuss G. 1997. The SMN-SIP1 complex has an essential role in spliceosomal snRNP biogenesis. Cell 90:1023–1029.

Gall JG. 2000. Cajal bodies: the first 100 years. Annu Rev Cell Dev Biol 16:273–300.

Gall JG, Bellini M, Wu Z, Murphy C. 1999. Assembly of the nuclear transcription and processing machinery: Cajal bodies (coiled bodies) and transcriptosomes. Mol Biol Cell 10:4385–4402.

Goldschmidt RB, Steward O. 1992. Retrograde regulation of neuronal size in the enthorhinal cortex: consequences of the destruction of dentate gyrus granule cells with colchicine. Rest Neurol Neurosci 3:335–343.

Habets WJ, Hoet MH, de Jong BA, van der Kemp A, van Venrooij WJ. 1989. Mapping of B cell epitopes on small nuclear ribonucleoproteins that react with human autoantibodies as well as with experimentally-induced mouse monoclonal antibodies. J Immunol 143:2560–2566.

Hadjiolov AA. 1985. The nucleolus and ribosome biogenesis. Wien: Springer-Verlag.

Haggar RA. 1957. Behavior of the accessory body of Cajal during axon reaction. J Comp Neurol 108:269–283.

Hardin JW, Spicer SS, Green WB. 1969. The paranucleolar structure, accessory body of Cajal, sex chromatin and related structures in nuclei of rat trigeminal neurons: a cytochemical and ultrastructural study. Anat Rec 164:403–432.

Hatton WJ, von Bartheld CS. 1999. Analysis of cell death in the trochlear nucleus of the chick embryo: calibration of the optical disector counting method reveals systematic bias. J Comp Neurol 409:169–186.

Hervas JP, Villegas J, Crespo D, Lafarga M. 1980. Coiled bodies in supraoptic nuclei of the rat hypothalamus during the postnatal period. Am J Anat 159:447–454.

Hunt SP, Mantyh PW, Priestley JV. 1992. The organization of biochemically characterized sensory neurons. In: Scott SA, editor. Sensory neurons: diversity, development and plasticity. New York: Oxford University Press. p 60–76.

Janevski J, Park PC, De Boni U. 1997. Changes in morphology and spatial position of coiled bodies during NGF-induced neuronal differentiation of PC12 cells. J Histochem Cytochem 45:1523–1531.

Jansen RP, Hurt EC, Kern H, Lehtonen H, Carmo-Fonseca M, Lapeyre B, Tollervey D. 1991. Evolutionary conservation of the human nucleolar protein fibrillarin and its functional expression in yeast. J Cell Biol 113:715–729.

Jones KJ, LaVelle A. 1986. Ultrastructural changes in the nucleoplasm of hamster facial neurons during a postnatal maturation period. Brain Res 377:119–126.

Kano Y, Maeda S, Sugiyama T. 1976. The localization of ribosomal cistrons (rDNA) in chromosomes of the rat. Chromosoma 55:37–42.

Kinderman NB, LaVelle A. 1976. A nucleolus-associated coiled body. J Neurocytol 5:545–550.

Lafarga M, Hervas JP, Santa-Cruz MC, Villegas J, Crespo D. 1983. The accessory body of Cajal in the neuronal nucleus. A light and electron microscopy approach. Anat Embryol (Berl) 166:19–30.

Lafarga M, Andres MA, Berciano MT, Maquiera E. 1991. Organization of nucleoli and nuclear bodies in osmotically stimulated supraoptic neurons of the rat. J Comp Neurol 308:329–339.

Lafarga M, Andres MA, Fernandez-Viadero C, Villegas J, Berciano MT. 1995. Number of nucleoli and coiled bodies and distribution of fibrillar centres in differentiating Purkinje neurons of chick and rat cerebellum. Anat Embryol (Berl) 191:359–367.

Lafarga M, Berciano MT, Garcia-Segura LM, Andres MA, Carmo-Fonseca M. 1998. Acute osmotic/stress stimuli induce a transient decrease of transcriptional activity in the neurosecretory neurons of supraoptic nuclei. J Neurocytol 27:205–217.

Lamond AI, Carmo-Fonseca M. 1993. The coiled body. Trends Cell Biol 3:198–204.

Lamond AI, Earnshaw WC. 1998. Structure and function in the nucleus. Science 280:547–553.

Lefebvre S, Bürglen L, Frezal J, Munnich A, Melki J. 1998. The role of the SMN gene in proximal spinal muscular atrophy. Hum Mol Genet 7:1531–1536.

Liu Q, Dreyfuss G. 1996. A novel nuclear structure containing the survival of motor neuron proteins. EMBO J 15:3555–3565.

Liu Q, Fischer U, Wang F, Dreyfuss G. 1997. The spinal muscular atrophy disease gene product, SMN, and its associated protein SIP1 are in a complex with spliceosomal snRNP proteins. Cell 90:1013–1021.

Macknight AD. 1988. Principles of cell volume regulation. Ren Physiol Biochem 11:114–141.

Magistretti PJ. 1999. Brain energy metabolism. In: Zigmond MJ, Bloom FE, Landis SC, Roberts JL, Squire LR, editors. Fundamental neuroscience. San Diego: Academic Press. p 389–416.

Matera AG. 1999. Nuclear bodies: multifaceted subdomains of the interchromatin space. Trends Cell Biol 9:302–309.

McClintock B. 1934. The relation of particular chromosomal elements to the development of nucleoli in Zea mais. Z Zellforsch 21:294–328.

McIlwain DL. 1991. Nuclear and cell body size in spinal motor neurons. In: Rowland LP, editor. Advances in neurology, vol. 56. Amyotrophic lateral sclerosis and other motor neuron diseases. New York: Raven Press. p 67–74.

Meier UT, Blobel G. 1994. NAP57, a mammalian nucleolar protein with a putative homolog in yeast and bacteria. J Cell Biol 127:1505–1514.

Mintz PJ, Spector DL. 2000. Compartmentalization of RNA processing factors within nuclear speckles. J Struct Biol 129:241–251.

Mintz PJ, Patterson SD, Newwald AF, Spahr CS, Spector DL. 1999. Purification and biochemical characterization of interchromatin granule clusters. EMBO J 18:4308–4320.

Misteli T, Caceres JF, Spector DL. 1997. The dynamics of a pre-mRNA splicing factor in living cells. Nature 387:523–527.

Modney BK, Hatton GI. 1989. Multiple synapse formation: a possible compensatory mechanism for increased cell size in rat supraoptic nucleus. J Neuroendocrinol 1:21–27.

Monneron A, Bernhard W. 1969. Fine structural organization of the interphase nucleus in some mammalian cells. J Ultrastruct Res 27:266–288.

Pearson EC, Bates DL, Prospero TD, Thomas JO. 1984. Neuronal nuclei and glial nuclei from mammalian cerebral cortex. Eur J Biochem 144: 553–560.

Pena E, Berciano MT, Fernandez R, Crespo P, Lafarga M. 2000. Stress-induced activation of c-Jun N-terminal kinase in sensory ganglion neurons: accumulation in nuclear domains enriched in splicing factors and distribution in perichromatin fibrils. Exp Cell Res 256:179–191.

Peters A, Palay SL, Webster H deF. 1991. The fine structure of the nervous system. Neurons and their supporting cells. New York: Oxford University Press.

Rambourg A, Clemont Y, Beaudet A. 1983. Ultrastructural features of six types of neurons in rat dorsal root ganglia. J Neurocytol 12:47–66.

Raska I, Ochs RL, Andrade LE, Chan EKL, Burlingame R, Peebles C, Gruol D, Tan EM. 1990. Association between the nucleolus and the coiled body. J Struct Biol 104:120–127.

Reimer G, Pollard KM, Penning CA, Ochs RL, Lischwe NA, Tan EM. 1987. Monoclonal antibody from (New Zealand Black x New Zealand White) F1 mouse and some human scleroderma sera target a Mr 34000 nucleolar protein of the U3-ribonucleoprotein particle. Arthritis Rheum 30: 793–800.

Sato S, Burgess SB, McIlwain DL. 1994. Transcription and motoneuron size. J Neurochem 63:1609–1615.

Schmidt EE, Schibler U. 1995. Cell size regulation, a mechanism that controls cellular RNA accumulation: consequences on regulation of the ubiquituous transcription factors Oct1 and NF-Y, and the liver-enriched transcription factor DBP. J Cell Biol 128:467–483.

Schwarzacher HG, Wachtler F. 1993. The nucleolus. Anat Embryol (Berl) 188:515–536.

Shaw PJ, Jordan EJ. 1995. The nucleolus. Annu Rev Cell Dev Biol 11:93–121.

Sleeman JE, Lamond AI. 1999. Nuclear organization of pre-mRNA splicing factors. Curr Opin Cell Biol 11:372–377.

Spector DL. 1993. Macromolecular domains within the cell nucleus. Annu Rev Cell Biol 9:265–315.

Wotherspoon G, Priestley JV. 1999. Expression of the 5-HT1B receptor by subtypes of rat trigeminal ganglion cells. Neuroscience 95:465–471.

Young PJ, Le TT, thi Man N, Burghes AH, Morris GE. 2000. The relationship between SMN, the spinal muscular atrophy protein, and nuclear coiled bodies in differentiated tissues and cultured cells. Exp Cell Res 256:365–374.

Zeng C, Kim E, Warren SL, Berget SM. 1997. Dynamic relocation of transcription and splicing factors dependent upon transcriptional activity. EMBO J 16:1401–1412.